

Self-Assembly | Very Important Paper |

VIP **Templated Chromophore Assembly on Peptide Scaffolds:
A Structural Evolution**Lou Rocard,^[a] Darren Wragg,^[b] Samuel Alexander Jobbins,^[b] Lorenzo Luciani,^[a]
Johan Wouters,^[c] Stefano Leoni,^[b] and Davide Bonifazi^{*[a]}

Abstract: The use of a template that bears pre-programmed receptor sites for selectively accommodating chromophores at given positions is an attractive approach for engineering artificial-light-harvesting systems. Indulging this line of thought, this work tackles the creation of tailored antenna architectures with yellow, red and blue chromophores, exploiting three dynamic covalent reactions simultaneously, namely disulfide exchange, acyl hydrazone, and boronic ester formations. The effect of various structural modifications, such as the chromophores as well as their spatial organization (distance, orientation, order) on the energy transfer within the antennas was studied by means of steady-

state UV/Vis absorption and fluorescence spectroscopies. This systematic study allowed for a significant improvement of the energy-transfer efficiencies to a noticeable 22 and 15% for the yellow and red donors, respectively, across the chromophores to the blue acceptor. Metadynamics simulations suggested that the conformational properties of the antennas are driven by intramolecular chromophoric stacking interactions that, upon forcing the α -helix to fold on itself, annul any effects deriving from the programming of the spatial arrangement of the receptor sites in the peptide backbone.

Introduction

Energy is the biggest issue of our current time.^[1] Despite the very abundant and sustainable source of energy available from sunlight, nowadays only a tiny fraction of the solar energy is used by thermal collectors and solar panels to generate heat and electricity. Artificial systems usually adsorb a fraction of the solar spectrum, whereas natural photosystems can collect a much larger energy fraction tailored by evolutionary selection.^[2] Hence, mimicking natural-light-harvesting (LH) systems^[3] to efficiently capture, transfer, and store energy is one of the most challenging tasks of the scientific community.^[4] In this respect, artificial antennas, with well-defined ordering of the dyes including interchromophoric distances, orientations, and ratio of donor-to-acceptor, can be developed.^[5] The supramolecular mixing of dyes,^[6] affording organogels,^[7] supramolecular polymers,^[8] co-crystals,^[9] metal-organic frameworks,^[10] is a very handy approach for engineering simple LH

systems (dyads) with high donor-to-acceptor ratios. On the other hand, the covalent assembly of dyes offers a controlled route as chromophores can be assembled into robust multidimensional architectures such as multilayers,^[11] dendrimers^[12] and macrocycles,^[13] through either static or dynamic covalent linkages,^[11d,e,14] allowing for the efficient light collection and energy-transfer control. Recently, the use of a pre-organized template (e.g., proteins,^[15] nucleic acids,^[15a,16] micelles,^[17] inorganic scaffolds)^[18] to organize distinct chromophores has been widely explored for light harvesting. Considering its versatility, this strategy appears to be very attractive for engineering multichromophoric antennas displaying controlled spatial organization and color distribution. In a recent endeavor, we reported the creation of a multichromophoric architecture through the use of a peptidic template Ac-QLA-X(**disulfide**)-QLAQLA-X(**hydrazide**)-QLAQLA-X(**diol**)-QLA-NH₂ **1** (X = modified amino acid), in which blue naphthalene-bisimide (B-NDI) **2**, red perylene-bisimide (R-PDI) **3** and yellow ethynylpyrene (Y-Py) **4** chromophores could be spatially organized through chemoselective reactions (Figure 1).^[19]

Specifically, the dye assembly was achieved by the simultaneous use of disulfide exchange, acyl hydrazone, and boronate-ester-formation reactions that took place at tailored receptor sites on the peptidic scaffold and allowed for the precise spatial programming of the chromophores. Although the proposed synthetic strategy is efficient and versatile to build multichromophoric architecture exhibiting any absorbed or emitted colors, the energy-transfer efficiencies (Φ_{ET}) within triad **5**, revealed to be as low as 5 and 5.5% for the Y-Py \rightarrow B-NDI and R-PDI \rightarrow B-NDI sensitization processes, respectively

[a] Dr. L. Rocard, L. Luciani, Prof. Dr. D. Bonifazi
School of Chemistry, Cardiff University
Park Place, CF10 3AT, Cardiff (UK)
E-mail: bonifazid@cardiff.ac.uk

[b] D. Wragg, Dr. S. A. Jobbins, Dr. S. Leoni
School of Chemistry, Cardiff University
Park Place, CF10 3AT, Cardiff (UK)

[c] Prof. Dr. J. Wouters
Department of Chemistry, University of Namur (UNamur)
61, rue de Bruxelles, Namur 5000 (Belgium)

 Supporting information and the ORCID identification number(s) for the author(s) of this article can be found under:
<https://doi.org/10.1002/chem.201803205>.

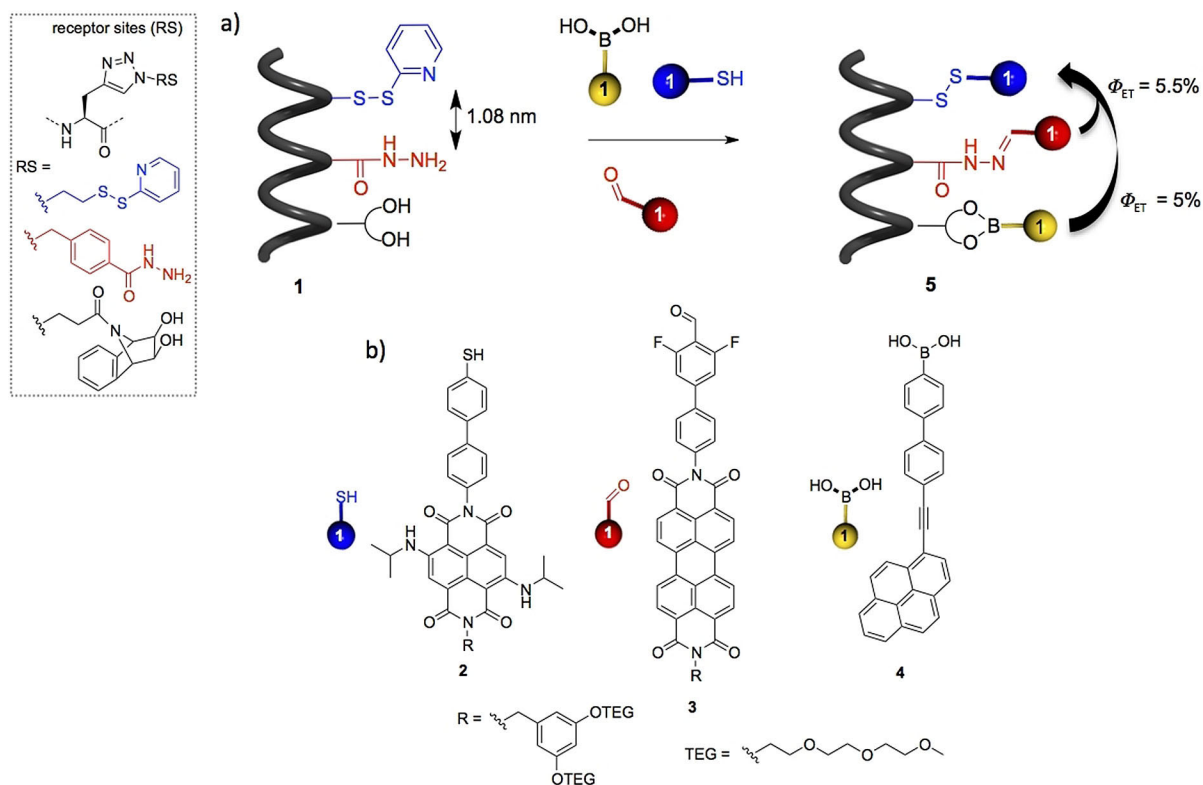


Figure 1. a) Simultaneous chromophoric assembly on pre-programmed peptide **1** (Ac-QLA-X(disulfide)-QLAQLA-X(hydrazide)-QLAQLA-X(diols)-QLA-NH₂) and energy-transfer efficiencies; b) chemical structure of the first generation of dyes bearing complementary sticky side.

(Figure 1). Thus, a structural modification of the system is required if one wants to enhance the Φ_{ET} values. Recalling the Förster theory, the rate of energy transfer k_T (FRET), defined by Equation (1), depends on the interchromophoric distances r and r_0 , the latter being the critical interchromophoric distance at which the energy-transfer efficiency is equal to 50%. The distance r_0 is calculated according to Equation (2)^[20]

$$k_{T(r)} = \frac{1}{\tau_D} \left(\frac{r_0}{r} \right)^6 \quad (1)$$

$$r_0 = 9.78 \times 10^3 [k^2 n^{-4} Q_D J(\lambda)]^{1/6} \text{ (in \AA)} \quad (2)$$

in which τ_D is the fluorescent lifetime of the donor in the absence of the acceptor, k^2 describes the transition dipole orientation, n is the refractive index of the medium, Q_D is the quantum yield of the donor fluorescence in the absence of the acceptor, and $J(\lambda)$ is the integral of the normalized spectral overlap between the donor emission and the acceptor absorption. Considering Q_D , $J(\lambda)$, r , and k^2 as the critical variables for improving Φ_{ET} in this work (Figure 2), we systematically studied the effect of: 1) dyes with enhanced spectral overlap between donor emission and acceptor absorption [$J(\lambda)$] and energy-donating chromophores with high emission quantum yields (Q_D); 2) different interchromophoric order, 3) distances (r) and 4) orientations (variation of dipole orientation factor k^2); 5) solvent.

Computational simulations of all the multichromophoric architectures in explicit solvent were performed to rationalize the conformational properties of the antennas. The use of molecular dynamics (MD) simulations allows for exquisite insight into the structure of the peptide and chromophores at the atomistic level, providing a means to generate and visualize the conformation of the architecture, usually corresponding to microstates associated with a particular energy basin. However, MD simulations are carried out on the femtosecond timescale, whereas the activated processes, such as the folding or unfolding of the peptide backbone, take place over nanosecond or even microsecond timescales. This means that unfeasibly long MD simulations would be required before any such event can be witnessed. Due to the coarse and complex nature of the underlying energy landscape of a real chemical system, the probability of transitioning from one energy basin to another is also very small. Without some form of acceleration, only states separated by barriers equal to or less than thermal fluctuations ($k_B T$) in the system are likely to be visited. To access other regions of the configuration space and to facilitate the crossing of larger barriers and the observation of critical events within a reasonable time frame, one must apply an enhanced sampling method.^[21] One such method of acceleration is metadynamics, the technique used in this work. In this technique, a history-dependent bias potential is iteratively built upon the underlying energy landscape. This discourages the system from returning to previously visited configurations and enables the systematic exploration of the configuration space. This

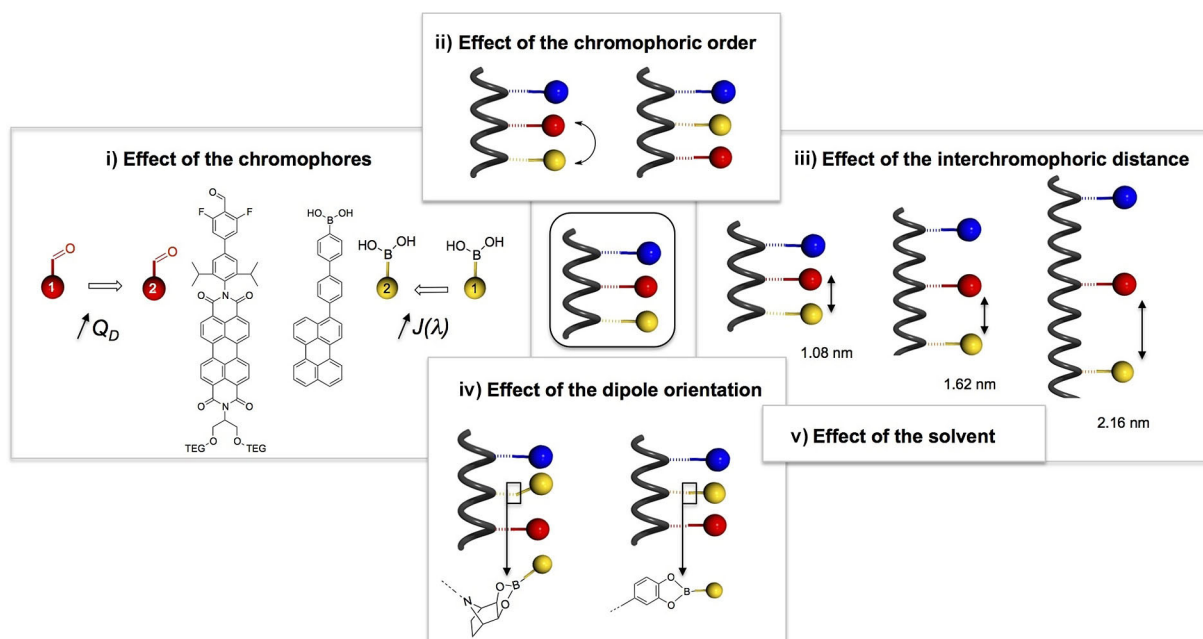


Figure 2. En route towards the structural evolution proposed in this study: i) effect of the chromophores; ii) effect of the chromophoric order; iii) effect of the interchromophoric distance; iv) effect of the dipole orientation; v) effect of the solvent.

allows for the induction and observation of structural changes, such as the folding and unfolding of the peptide backbone, which would not be possible by standard MD simulations alone (see Supporting Information for the details).^[22]

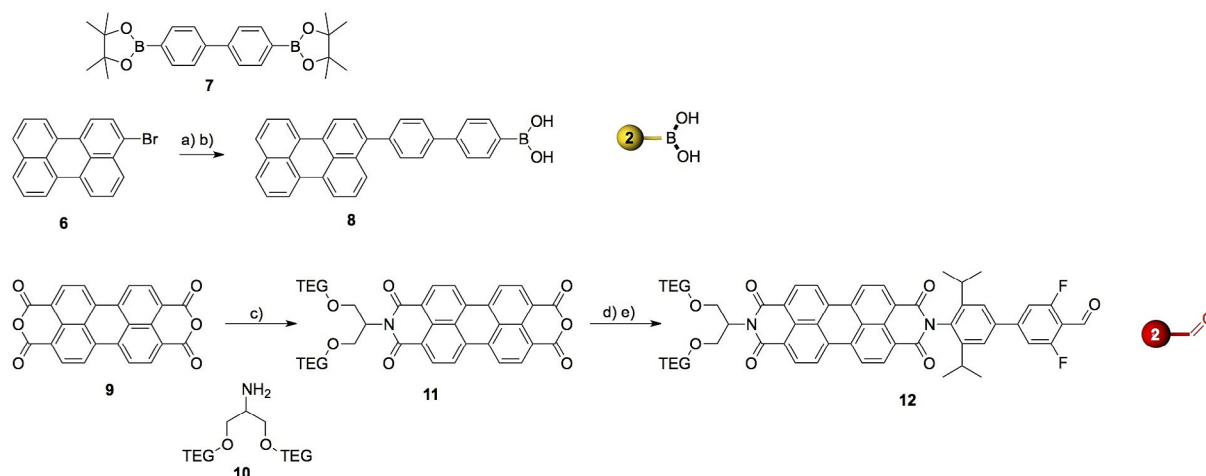
Results and Discussion

Development of a new generation of chromophores

Following the photophysical characterization of the previously engineered antenna **5**, we recognized that the emission profile of the pyrene moiety (Y-Py **4**) does not best match the UV/Vis absorption of the perylene bisimide module (R-PDI **3**). Accordingly, ethynylpyrene Y-Py **4** has been substituted by a perylene chromophore (Y-Per) because the latter displays a low-energy emission profile. The optical properties of the perylene^[23] make it a suitable candidate for our architecture because it strongly absorbs in the blue region ($\epsilon = 38\,500 \text{ L mol}^{-1} \text{ cm}^{-1}$ at 434 nm), and it is highly fluorescent with a small Stokes shift.^[24] In parallel, we also decided to amend the structure of the red chromophore because the R-PDI **3** showed a very low fluorescence quantum yield (QY, < 4%). Although the perylene bisimide and its derivatives are known to be highly fluorescent (QY > 90%),^[25] electron-rich *N*-benzyl substituent can undergo photo-induced electron transfer to the PDI core,^[25,26] thus quenching the emission of the singlet excited state. Hence, we envisaged an aliphatic linker group at the *N*-atom, in which the solubilizing triethylene glycol (TEG) chains are attached. It is worth noting that the 2,6-diisopropylphenyl substituent was also introduced to prevent parasite interchromophoric π - π stacking within the antenna.^[27] Thus, we prepared chromophores Y-Per **8** and R-PDI **12** (Scheme 1).

For the synthesis of Y-Per **8**, a Pd-catalyzed Suzuki cross-coupling was carried out between bromo-erylene **6**^[28] and 4,4'-biphenyldiboronic acid (bis)pinacol ester **7** in the presence of [Pd(PPh₃)₄] and K₂CO₃ to afford the corresponding boronic ester in 72% yield. The subsequent removal of the pinacol protecting group by oxidative cleavage with NaIO₄ and treatment with a 1 M aqueous solution of HCl, afforded the desired boronic acid Y-Per **8** in 90% yield (Scheme 1).^[29] As far as R-PDI **12** is concerned, monoanhydride intermediate **11** was obtained as a solid through a mono-condensation reaction between the perylene dianhydride (PDA) and amine **10**^[30] in a water/isopropanol mixture at 120 °C for ten days, a method reported by Mattern and co-workers.^[31] The second condensation reaction with 4-bromo-2,6-diisopropylaniline was subsequently carried out in propionic acid at 140 °C for 7 h under microwave irradiations affording unsymmetrical PDI in 38% over two steps. Pd-catalyzed Suzuki cross-coupling of the latter compound with 3,5-difluoro-4-formylphenyl boronic acid afforded final R-PDI **12** (Scheme 1). As expected, the dyes Y-Per **8** and R-PDI **12** exhibited remarkably high QY of 70 and 94%, respectively, with the emission profile of Y-Per **8** showing excellent spectral complementarity with the absorption spectrum of R-PDI **12** (Figure 3b). Notably, the total absorption envelop of the dyes shows a good matching with the solar spectrum (Figure 3a,b).

Following the self-assembly methodology previously developed by us,^[19] the dyes were assembled on α -helix peptide **1** bearing the three-receptor sites every (*i*, *i* + 7) residues. Multichromophoric architecture **13** was prepared with dyes 1) Y-Per **8**, R-PDI **3**, and B-NDI **2**, as well as **14** with 2) Y-Per **8**, R-PDI **12**, and B-NDI **2**, in anhydrous DMF over 4 h in the presence of a catalytic amount of *m*-phenylenediamine (*m*PDA) and peptide **1** (Figure 4). After purification, the chemical identities of desired antennas **13** and **14** were confirmed by MALDI-TOF anal-



Scheme 1. Synthesis of Y-Per **8** and R-PDI **12**; a) K_2CO_3 , $[\text{Pd}(\text{PPh}_3)_4]$, 1,4-dioxane/ H_2O , 85°C , 3 h, 72%; b) i) NaIO_4 , THF/ H_2O (4 : 1), RT, 1 h 30, ii) HCl (1 M), RT, 20 h, 90%; c) i) amine **10**, Et_3N , $i\text{PrOH}/\text{H}_2\text{O}$, 120°C , 10 d, ii) 5% HCl (aq), 120°C , 10 min, not isolated; d) 4-bromo-2,6-diisopropylaniline, propionic acid, microwave irradiation, 140°C , 7 h, 38% over two steps; e) 3,5-difluoro-4-formylphenyl boronic acid, K_2CO_3 , $[\text{Pd}(\text{PPh}_3)_4]$, 1,4-dioxane/ H_2O , 80°C , 20 h, 90%.

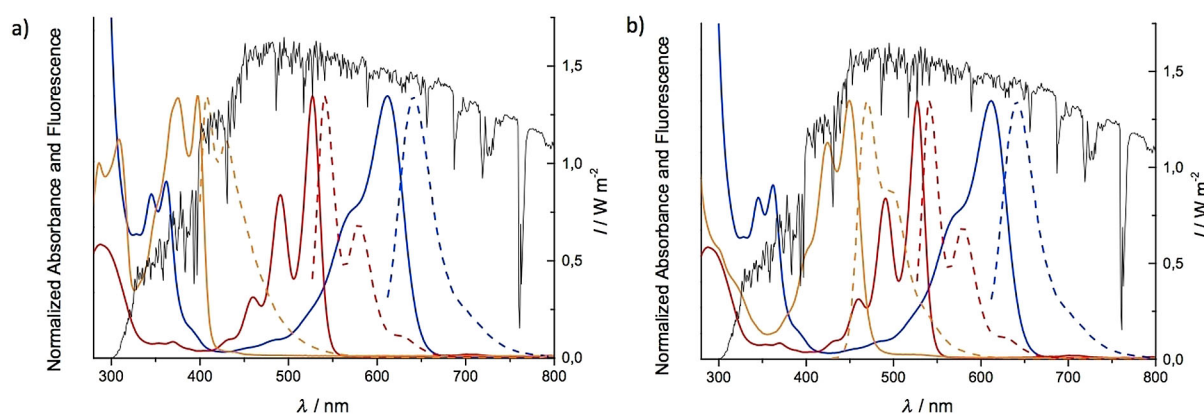


Figure 3. Normalized absorption (solid) and fluorescence (dashed) spectra of colored dyes a) 1st generation: Y-Py **4** (yellow), R-PDI **3** (red), B-NDI **2** (blue) and b) 2nd generation: Y-Per **8** (yellow), R-PDI **12** (red), B-NDI **2** (blue) in DMF plotted against the solar spectrum.

yses (see Supporting Information). Antennas **13** and **14** were analyzed by UV/Vis absorption spectroscopy in DMF solution. The spectra were compared with the arithmetic sum of the three independent dye absorptions after normalization on the B-NDI maximum at 612 nm. Characteristic bands of the three dyes were observed but a significant hypochromism for R-PDI-centered bands was noticed, suggesting a non-quantitative introduction of the R-PDI moiety due to steric hindrance and π - π stacking interactions.

Steady-state fluorescence measurements were performed to determine the energy-transfer (ET) efficiencies Φ_{ET} following two methods (see also Supporting Information). Method A involved calculating $\Phi_{\text{ET}} = QY_{\text{B-NDI}}^* / QY_{\text{B-NDI}}$, the ratio of quantum yields of acceptor B-NDI within YRB peptide ($QY_{\text{B-NDI}}$) upon selective excitation of the donor units R-PDI ($\lambda_{\text{exc}} = 495$ nm) or Y-Per ($\lambda_{\text{exc}} = 423$ nm) and $QY_{\text{B-NDI}}$ upon direct excitation ($\lambda_{\text{exc}} = 609$ nm). In Method B, the calculation was performed by using $\Phi_{\text{ET}} = E_{\text{X}_D} / A_{\text{D}}$, in which E_{X_D} and A_{D} are the fluorescence and absorption intensities of the donor in the normalized excitation and absorption spectra, respectively, with the absorption and

excitation spectra normalized at the maximum absorption wavelength of blue chromophore unit B-NDI ($\lambda_{\text{max}} = 612$ nm). For antenna **13**, $\Phi_{\text{ET}}^{(\text{Y-Per} \rightarrow \text{B-NDI})}$ and $\Phi_{\text{ET}}^{(\text{R-PDI} \rightarrow \text{B-NDI})}$ were estimated to be 7.7 and 7.7% with Method A and 7 and 7.2% with Method B, respectively. Alternatively, $\Phi_{\text{ET}}^{(\text{Y-Per} \rightarrow \text{B-NDI})}$ and $\Phi_{\text{ET}}^{(\text{R-PDI} \rightarrow \text{B-NDI})}$ values of 3.7 and 19% in antenna **14** have been measured by Method A and these were found to be very close to those obtained by Method B (3.2 and 17.9%). A significant improvement for $\Phi_{\text{ET}}^{(\text{R-PDI} \rightarrow \text{B-NDI})}$ was observed when using R-PDI **12** from 5.5 and 7.7% for antennas **5** and **13** to 19% for architecture **14**. Metadynamics simulations of architecture **14** (Figure 5, see Supporting Information for free energy surface) showed that the peptide backbone is essentially folded as an α -helix, with some distortion at the nitrogen-terminal end. Notably, the PDI and NDI cores are facing to each other, whereas the perylene moiety hardly faces the other two chromophoric modules in any of the calculated conformations. The perylene core seems to mostly interact with the diphenyl spacers instead. The lack of any relevant face-to-face PDI/peryene and NDI/peryene conformations is likely to be the cause of the

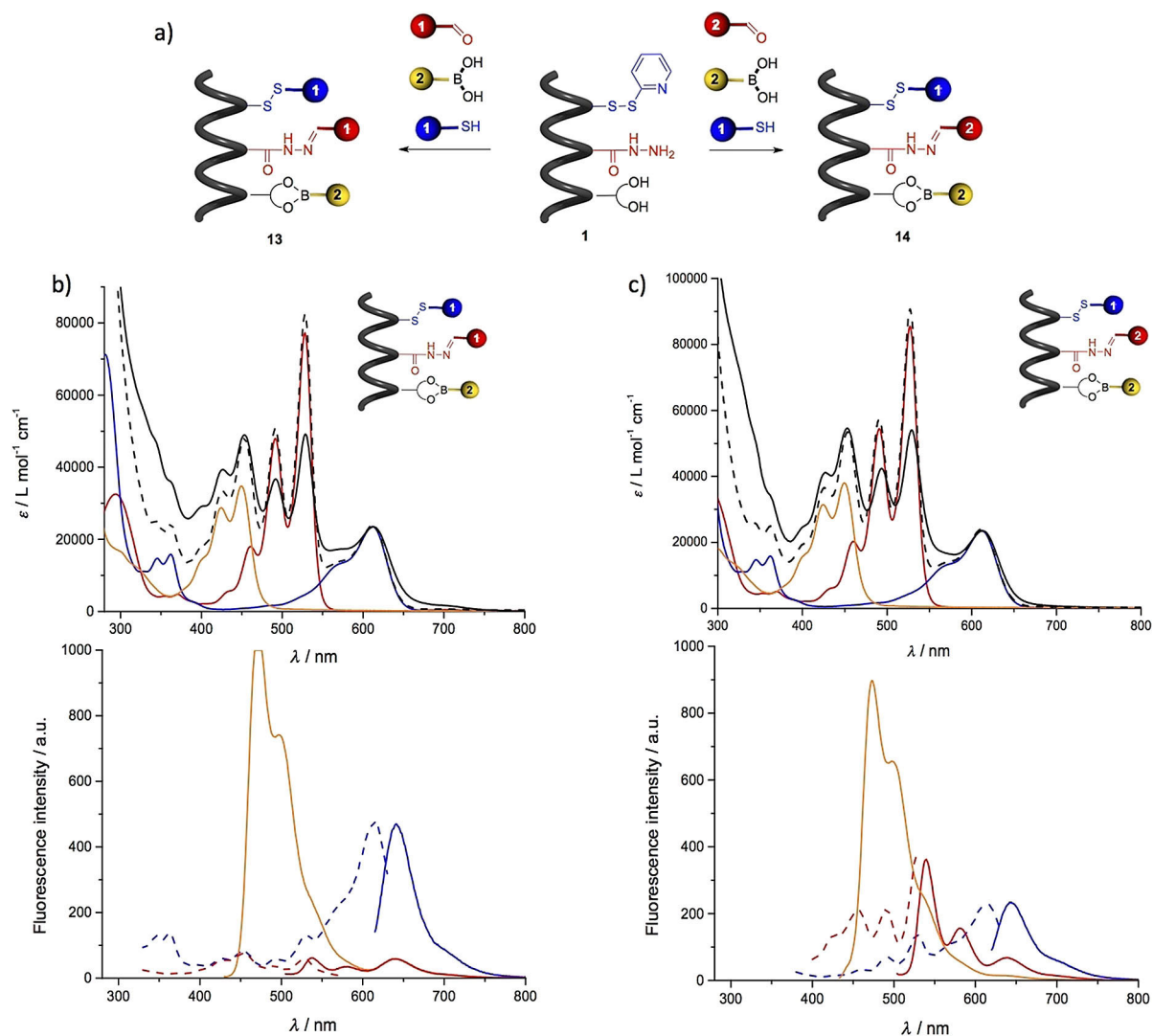


Figure 4. Colored assembly with B-NDI 2, R-PDI 3 or 12 and Y-Per 8 on peptidic scaffold 1; a) *m*PDPA, DMF, RT, 4 h. Middle: Absorption spectra of b) YRB peptide 13 (solid black line) and c) YRB peptide 14 (solid black line) normalized with arithmetic sum (dashed line) of absorption of dyes B-NDI 2, R-PDI 3 or 12, Y-Per 8 in DMF on B-NDI unit. Bottom: Emission (solid lines: $\lambda_{exc} = 423$ nm in yellow, $\lambda_{exc} = 495$ nm in red, $\lambda_{exc} = 612$ nm in blue), and corresponding normalized excitation spectra (dashed lines: $\lambda_{emis} = 540$ nm in red, $\lambda_{emis} = 640$ nm in blue) of peptides b) 13, c) 14.

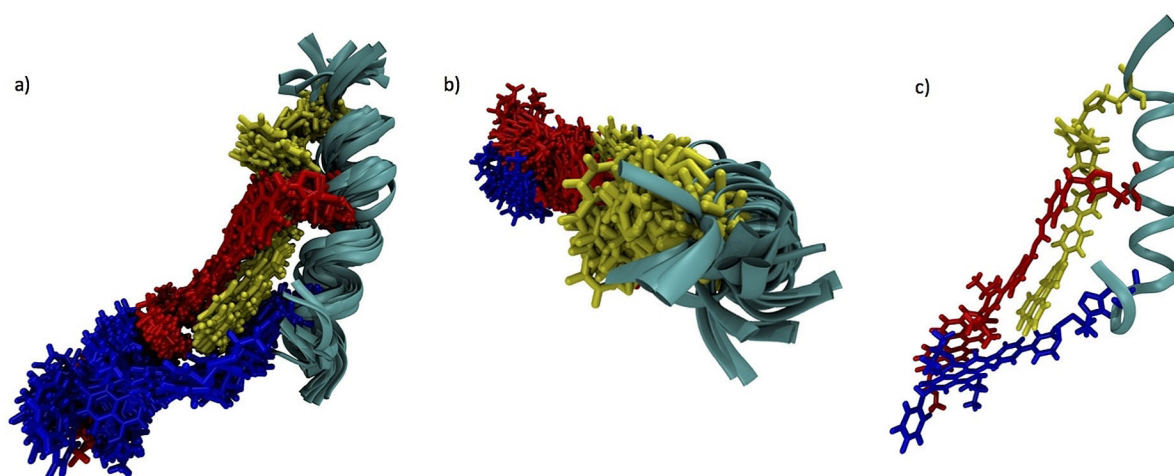


Figure 5. Metadynamics simulations of antenna 14 (100 ns); a) side and b) top view of overlaid frames; c) most stable conformation.

poor FRET between the perylene unit and the other chromophores.

Variation of the interchromophoric distance (r) and the dipole orientation

In a parallel avenue, we investigated the effect of the interchromophoric distance. Considering that too short interchromophoric distances might prevent the quantitative linkage of the PDI moiety and favor quenching mechanisms other than energy transfers, we decided to prepare peptide templates featuring a receptor site at every ($i, i + 10$) and ($i, i + 14$) residues, corresponding to three (peptide **15**) and four (peptide **16**) turns of α -helix, respectively (Figure 6). Considering that peptide Ac-QLA-X(disulfide)-QLAQLA-X(hydrazide)-QLAQLA-X(diol)-QLA-NH₂ **1** features a receptor site at every ($i, i + 7$) residues with a space distance of 1.08 nm in its folded conformation, peptides **15** and **16** should lead to antenna with interchromophoric distances of 1.62 and 2.16 nm (pitch of α -helix = 0.54 nm), respectively.^[32] The longer interchromophoric distance might enhance the ET because it is known that maximum FRET efficiencies are observed for interchromophoric distances between 1 and 3 nm.^[33] In addition, we were also inter-

ested in studying the impact of the ordering of the chromophores on both the yield of the assembly and Φ_{ET} . In particular, we wanted to investigate the effect of the bidirectional (R-PDI \leftarrow Y-Per \rightarrow B-NDI) vs. Y-Per \rightarrow R-PDI \rightarrow B-NDI) cascaded, or direct energy transfers.

Thus, three newly designed pre-programmed peptides were synthesized (Scheme 2) by solid phase peptide syntheses (SPPS)^[32] following Fmoc/tBu strategy and terminal *N*-capping: a 27-mer: Ac-QLA-X(disulfide)-QLAQLAQLA-X(hydrazide)-QLAQLAQLA-X(diol)-QLA-NH₂ **15**, a 35-mer: Ac-QLA-X(disulfide)-QLAQLAQLAQLAQLA-Q-X(hydrazide)-QLAQLAQLAQLAQLA-Q-X(diol)-QLA-NH₂ **16** and a new 21-mer: Ac-QLA-X(disulfide)-QLAQLA-X(diol)-QLAQLA-X(hydrazide)-QLA-NH₂ **17**. The resin cleavage and side-chain deprotection were simultaneously performed in the presence of trifluoroacetic acid (TFA)/triisopropylsilane (TIS)/H₂O/ethanedithiol (EDT) (94:1:2.5:2.5). The disulfide entities were subsequently introduced in solution by disulfide exchange with 2,2'-dipyridyl disulfide and diisopropylethylamine (DIEA) to afford the targeted peptides. After purification of the materials by RP-HPLC (see Supporting Information), the chemical identity of the peptides was confirmed by ESI-MS(Q-TOF). Simultaneous assembly of the chromophores onto peptides **15**, **16**, and **17** gave antennas **21**, **22**, and **23**, respective-

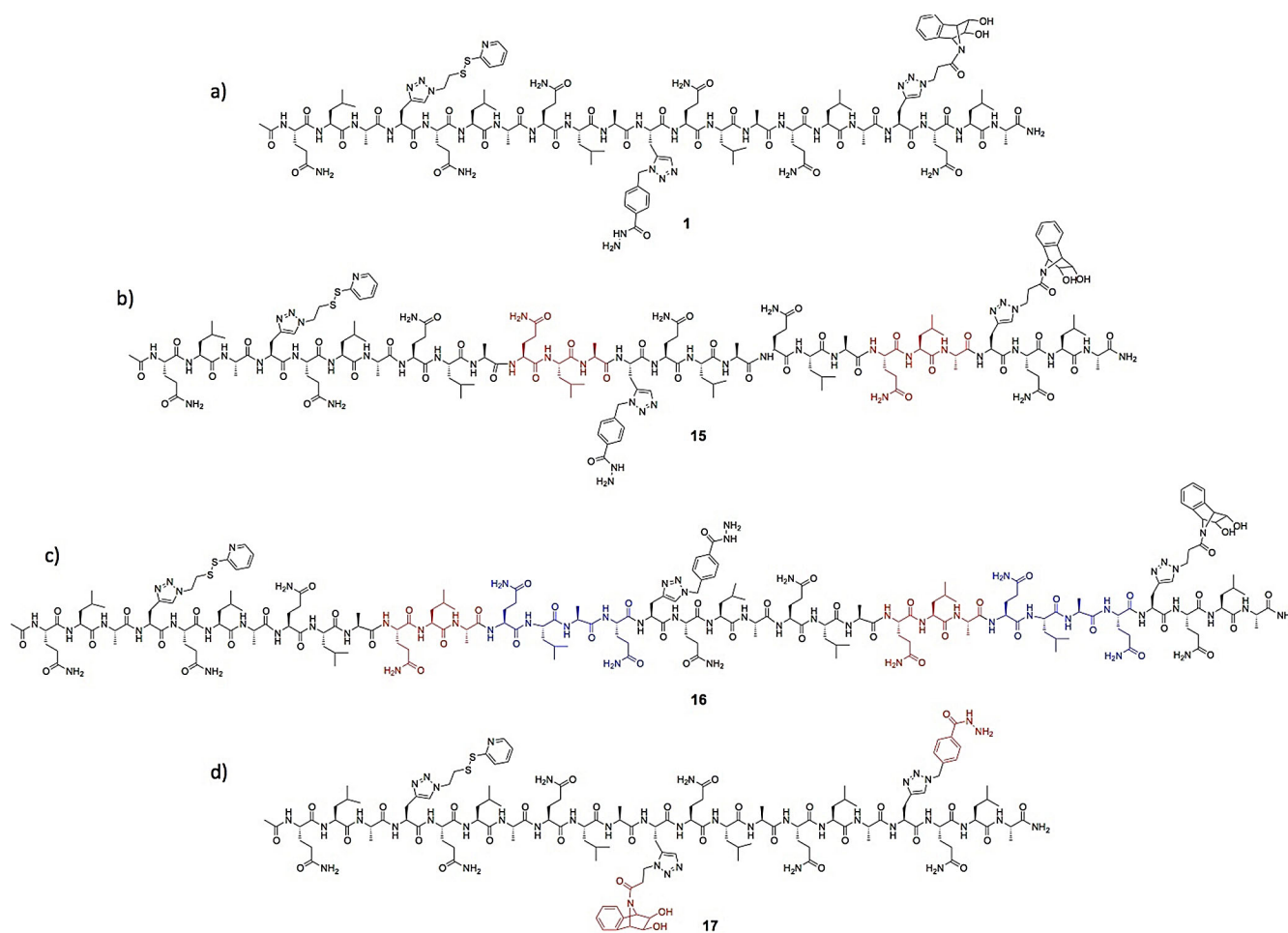
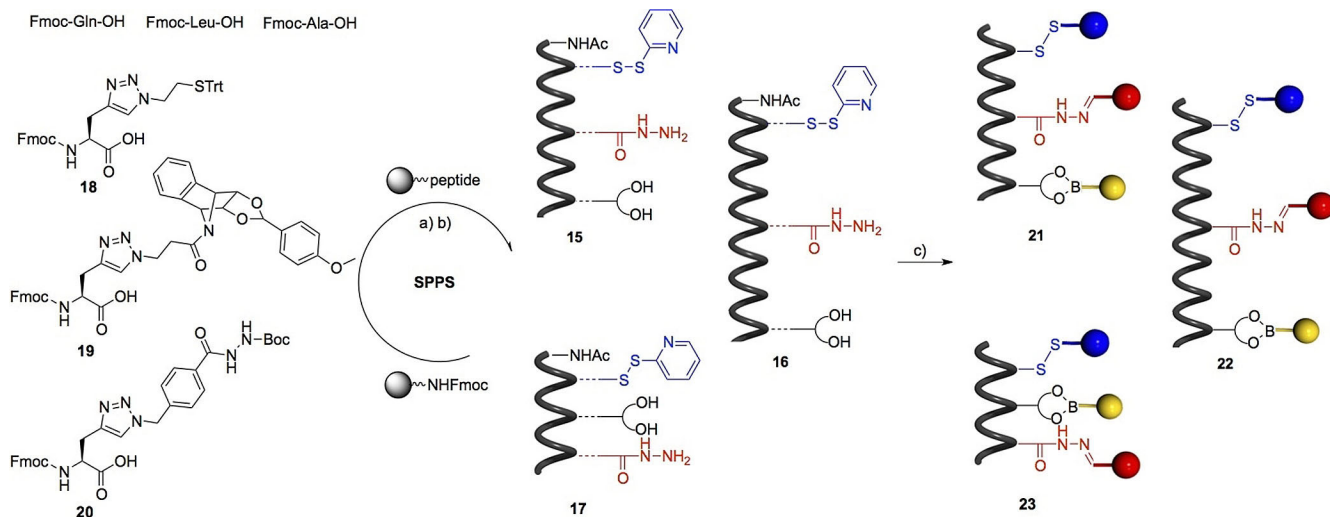


Figure 6. Structures of peptides a) **1**, b) **15**, c) **16** in which receptor sites are separated by 1.08, 1.62 and 2.16 nm, respectively; d) peptide **17** in which the order of the diol and hydrazide receptor sites is switched.



Scheme 2. Synthesis of the antennas; a) SPPS: i) Fmoc deprotection: 20% piperidine in DMF, RT, 3×6 min; ii) AA coupling: Fmoc-AA-OH, HATU, DIEA, DMF/*N*-methyl-2-pyrrolidone (NMP), RT, 25 min; iii) Ac₂O/pyridine/NMP (1:2:2), 2×15 min; iv) TFA/TIS/H₂O/EDT (94:1:2.5:2.5), RT, 2 h; b) 2,2'-dipyridyl disulfide, DIEA, DMF, 1 h; c) Simultaneous assembly with B-NDI 2, R-PDI 12 and Y-Per 8, *m*PDA, DMF, 4 h, RT.

ly, following the protocol described previously (Scheme 2). The multichromophoric architectures were purified by size-exclusion chromatography (SEC) and characterized by MALDI-TOF mass spectrometry.

The absorption spectra, normalized with the arithmetic sum of the absorption spectra of the three free dyes, interestingly displayed three different UV/vis profiles (Figure 7, top). A good overlapping between the two spectra was observed for antenna 23, whereas hypochromism for the R-PDI-centered bands (compared to the arithmetic sum of the spectra of the dyes) was noticed for antennas 21 and 22, similarly to the cases of

13 and 14. The measured energy-transfer efficiencies are listed in Table 1. Notably, increasing the distance between the chromophores did not significantly perturbate the Φ_{ET} values because $\Phi_{ET}^{(Y-Per \rightarrow B-NDI)}$ was determined to be around 3% for antennas 21–22, whereas $\Phi_{ET}^{(R-PDI \rightarrow B-NDI)}$ was 18% in the three cases. The change of the order within antenna 23 slightly improved ET efficiencies ($\Phi_{ET}^{(Y-Per \rightarrow B-NDI)}$ and $\Phi_{ET}^{(R-PDI \rightarrow B-NDI)}$ estimated to be 7.7 and 21.9% with Method A; and 7.4 and 21.8% with Method B) despite the bidirectional character of the ET process.

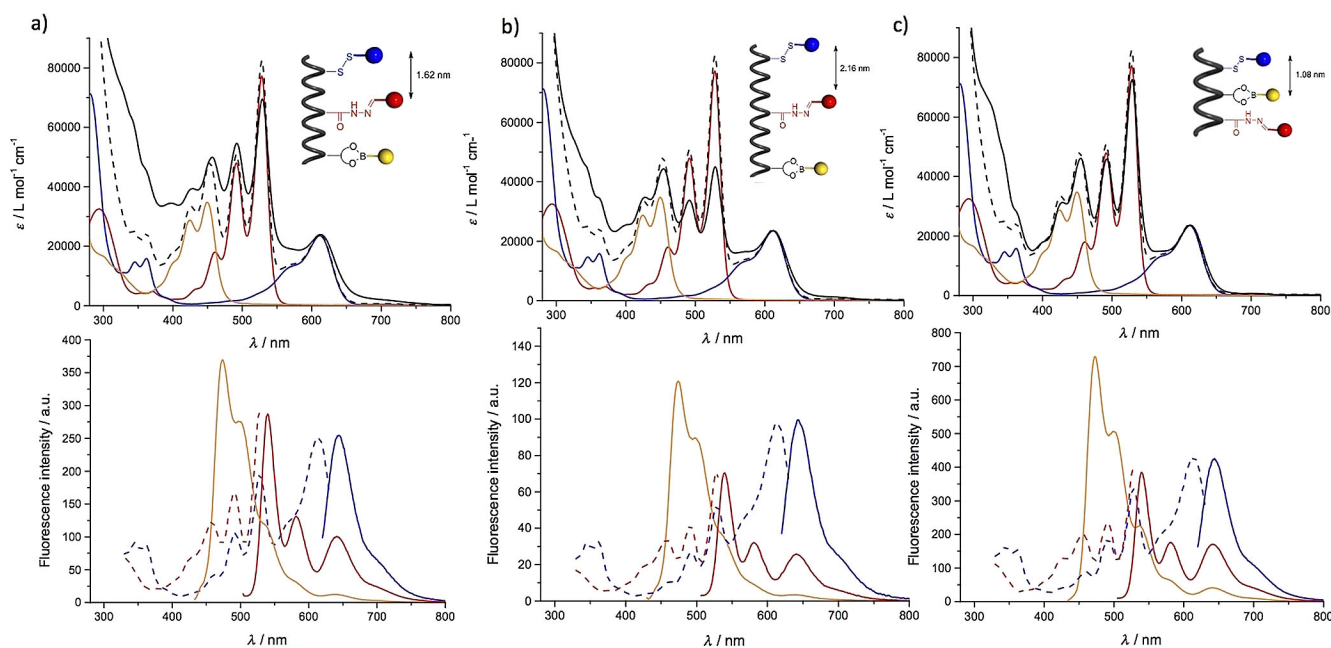


Figure 7. Top: Absorption spectra of antennas (solid black line) a) 21, b) 22, c) 23 normalized with the arithmetic sum of dyes (dashed black line) B-NDI 2, R-PDI 12, Y-Per 8 on B-NDI in DMF. Bottom: Emission (solid lines: $\lambda_{exc} = 423$ nm in yellow, $\lambda_{exc} = 495$ nm in red, $\lambda_{exc} = 612$ nm in blue), and corresponding normalized excitation spectra (dashed lines: $\lambda_{emis} = 540$ nm in red, $\lambda_{emis} = 640$ nm in blue) of antennas a) 21, b) 22, c) 23.

Table 1. Energy-transfer efficiencies.

Entry	Peptide	Dyes distance [nm]	Methods	$\Phi_{ET}^{(Y-Per \rightarrow B-NDI)}$ [%]	$\Phi_{ET}^{(R-PDI \rightarrow B-NDI)}$ [%]
1	YRB 14	1.08	A: $\Phi_{ET} = QY_{B-NDI}^*/QY_{B-NDI}$	3.7	17.9
			B: $\Phi_{ET} = EX_D/A_D$	3.2	19
2	YRB 21	1.62	A	2.7	17
			B	2.9	17
3	YRB 22	2.16	A	2.5	19.1
			B	2.5	18.5
4	RYB 23	1.08	A	7.7	21.9
			B	7.4	21.8
5	RYB 30 ($n=1$)	1.08	A	4.2	18
			B	4	17.4
6	RYB 31 ($n=3$)	1.08	A	4.7	16.6
			B	4.6	16.2

The metadynamics calculations shown in Figure 8 clearly displayed that the energy profile is dominated by a minimum, in which the three chromophores are strongly interacting to each other in the case of antenna **21**. In contrast to antenna **14**, the perylene and NDI cores are facing to each other, whereas the PDI core is pointing in another direction. Surprisingly, when the distance between the receptor sites was increased to 2.16 nm as in the case of **22**, the strong intramolecular stacking interaction between the different chromophores (with broader spatial occupancies) led to a strong distortion of the helical structure of the peptidic backbone. This finding suggests that the main driving force ruling the conformation of the peptide backbone is the interchromophoric stacking and not the opposite (i.e., the peptide template).

On the one hand, the interchromophoric interactions annul the effect of the distances between the receptor sites in the antennas, in agreement with the experimental findings for which the Φ_{ET} values are very similar for antennas **14**, **21**, and **22**. On the other hand, when the R-PDI unit is placed at terminus of the peptide (e.g., antenna **23**), the deepest minimum in the energy profile corresponds to a largely α -helical structure. The folding of the flexible linker of the receptor sites led again to a strong interchromophoric stacking, in particular between the perylene and PDI cores in the case of **23**.

Replacement of the linker (orientation of the dipoles) and solvent effects

As clearly displayed in the metadynamics simulations of all antennas, the non-planar bicyclic diol anchor forces the boronic ester to adopt an unfavorable conformation, for which the Y-Per core points in another direction with respect to that of chromophores R-PDI and B-NDI (Figure 5). Indeed, when looking at the crystal structures of diol-based sticky side precursors **24** and **25** (Figure 9), one can easily recognize that the diol functional group sits on a different plan than that of the linker, thus in net contrast to the directional properties of the other receptor sites. This results in an unfavorable pre-organization of the architecture, preventing the chromophores to adopt face-to-face conformations. Thus, we conjectured that the non-planar bicyclic diol site could be replaced by a catechol-based

linker. We investigated two catechol derivatives, of which one was rigid, with only one sp^3 carbon between the catechol and the triazole (see amino acid precursor **26**, Scheme 3), and a second featuring three sp^3 carbons as the linker (see amino acid precursor **27**, Scheme 3).

Accordingly, two Fmoc-protected catechol-containing amino acids **26** and **27** were synthesized (see Supporting Information) and used to prepare the peptides Ac-QLA-X(**disulfide**)-QLAQLA-X(**catechol**)-QLAQLA-X(**hydrazide**)-NH₂ **28** and **29** following the RYB order (Scheme 3), which so far gave the best Φ_{ET} results. After purification, the chromophore assembly was performed following the standard protocol to give antennas **30** and **31**, respectively. The absorption spectra of **30** and **31** normalized with the arithmetic sum of the absorption of the dyes on the B-NDI profile are shown in Figure 10a,b (top).

If compared to RYB peptide **23**, the measured energy-transfer efficiencies for the new antennas are lower; $\Phi_{ET}^{(R-PDI \rightarrow B-NDI)}$ is around 18 and 16% for **30** and **31**, respectively; $\Phi_{ET}^{(Y-Per \rightarrow B-NDI)}$ is around 4 and 5% for **30** and **31**. The metadynamics analysis for antenna **31** is depicted in Figure 11a–c. The peptide scaffold predominantly adopts an α -helical conformation, but the spatial occupancy of the dyes in antenna **31** is less confined than in the previous antenna architectures bearing the bicyclic diol. It is worth noting that some conformations for **31** exist, in which the Y-Per unit interacts in a face-to-face fashion with the other chromophore cores (Figure 11). However, due to the large flexibility of the linkers, this strategy does not seem to correctly pre-organize the dipole orientation of the dyes and does not dramatically enhance the energy-transfer processes.

Alternatively, the boronic ester linkage in catechol-based antennas **30** and **31** appears to be less stable than the one obtained from the bicyclic diol, due to the conjugation of the catechol moiety making it more Lewis acidic. We also assumed that the presence of traces of Me₂NH and water, coming from the thermal decomposition of DMF by the extrusion of CO, might catalyze the hydrolysis of the boronic ester linkage, especially under very dilute conditions (needed for the fluorescence measurements). The unleashing of free perylene dye in solution directly altered the $\Phi_{ET}^{(Y-Per \rightarrow B-NDI)}$ values. This consideration prompted us to look at an alternative solvent, such as

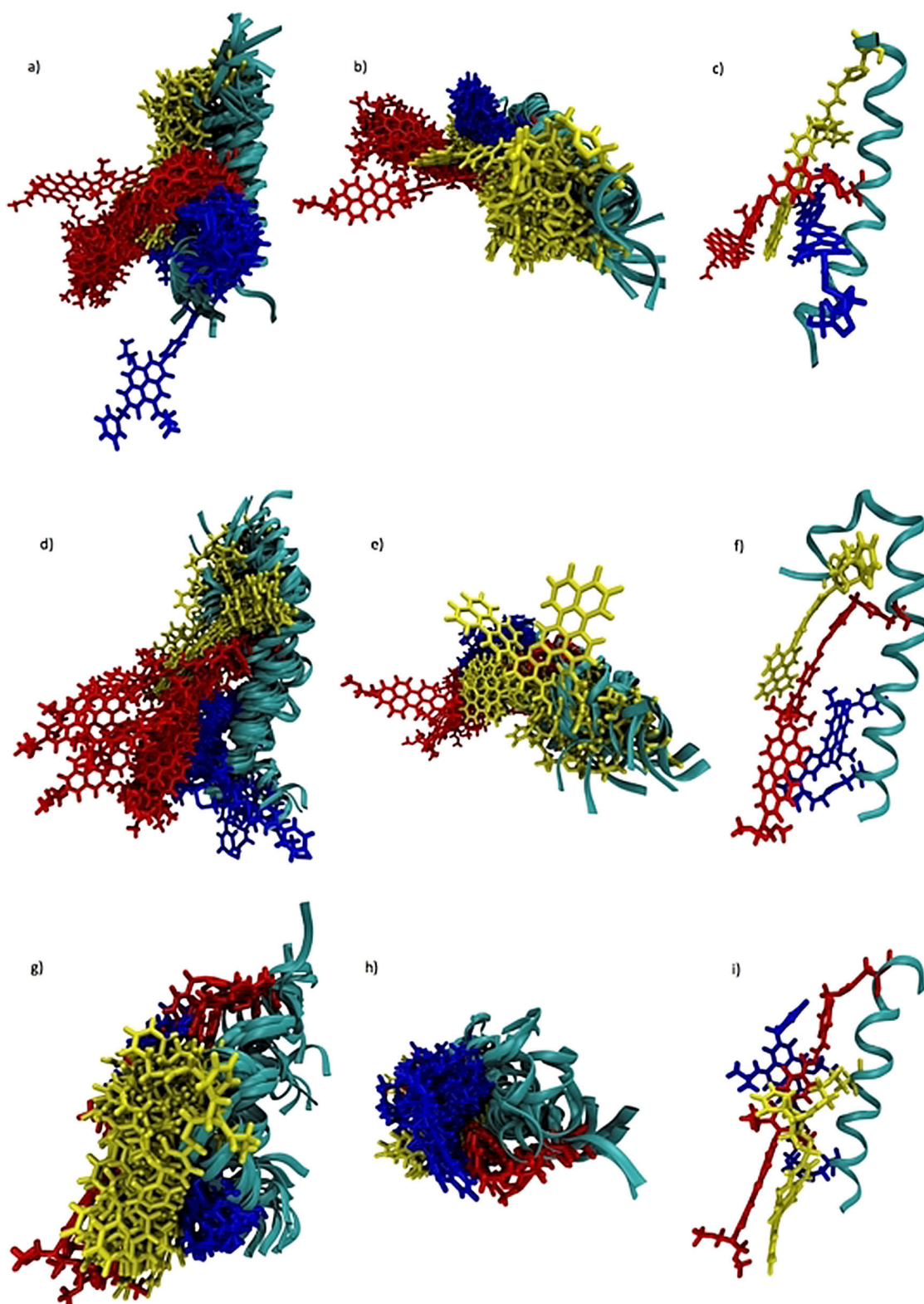


Figure 8. Metadynamics simulations (100 ns); a, d, g) side and b, e, h) top view of overlaid frames; c, f, i) most stable conformation of antennas **21**, **22**, **23** respectively.

dry *N,N*-dimethylacetamide (DMA). Accordingly, the assembly of the dyes was performed on Ac-QLA-X(disulfide)-QLAQLA-X(diols)-QLAQLA-X(hydrazide)-NH₂ **17** in distilled DMA to give antenna **23** after purification by SEC.

Normalized UV/Vis absorption spectrum of **23** in DMA shows a great correlation confirming the quantitative introduction of the chromophores as in the case of DMF (Figure 10 c, top). Finally, the fluorescence measurements were monitored

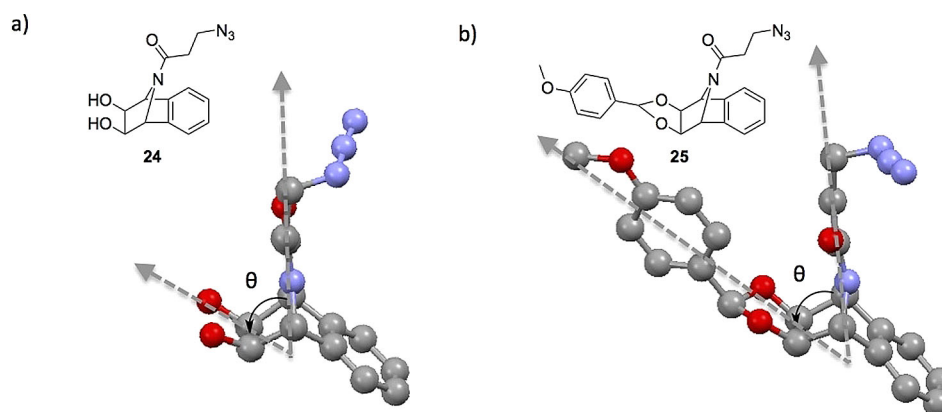
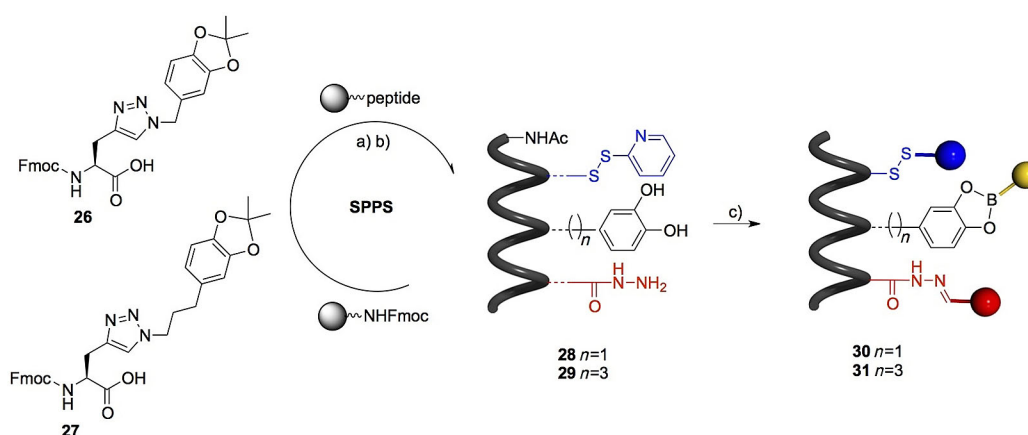


Figure 9. Side view of the crystal structures of a) diol **24** and b) protected diol **25**. Crystals were grown by slow evaporation from solutions in THF for **24** and EtOAc for **25**. Color code: grey (C), red (O) and blue (N).



Scheme 3. Synthesis of catechol based antennas; a) SPPS: i) Fmoc deprotection: 20% piperidine in DMF, RT, 3 × 6 min; ii) AA coupling: Fmoc-AA-OH, HATU, DIEA, DMF/NMP, RT, 25 min; iii) Ac₂O/pyridine/NMP (1:2:2), 2 × 15 min; iv) TFA/TIS/H₂O/EDT (94:1:2.5:2.5), RT, 2 h; b) 2,2'-dipyridyl disulfide, DIEA, DMF, 1 h; Chromophore assembly with B-NDI **2**, R-PDI **12** and Y-Per **8**, c) m-PDA, DMF, 4 h, RT.

in DMA and compared with those obtained in DMF (Figure 10c, bottom). Although $\Phi_{\text{ET}}^{(\text{R-PDI} \rightarrow \text{B-NDI})}$ was estimated to be 22% in both solvents, $\Phi_{\text{ET}}^{(\text{Y-Per} \rightarrow \text{B-NDI})}$ was determined to be around 15% (Table 2), a double value compared to that recorded in DMF. This finding further suggests that when boronic esters are used, one needs to carefully choose a suitable anhydrous solvent to avoid leakage of the chromophore in solution as a consequence of parasitic hydrolysis.

Conclusions

We have investigated α -helix peptides as templates to engineer antennas through a simultaneous multichromophoric assembly approach. Specifically, we systematically studied the effect of 1) dyes with enhanced spectral overlap between donor emission and acceptor absorption and energy-donating chromophores with high emission quantum yields; 2) different interchromophoric order, 3) distances (r) and 4) orientations and; 5) solvents. Replacing the ethynylpyrene chromophore bearing a perylene unit with the latter displaying better spectral overlaps between donor emission and acceptor absorption

as well as higher QY, revealed to have no major impact on the $\Phi_{\text{ET}}^{(\text{Y-Per} \rightarrow \text{B-NDI})}$. However, a significant improvement of $\Phi_{\text{ET}}^{(\text{R-PDI} \rightarrow \text{B-NDI})}$ (from 5 to about 20%) was observed with highly fluorescent PDI (QY = 94%). In a parallel avenue, we discovered that increasing the distance between the receptor sites on the peptide scaffold (from 1.08 to 1.62 and 2.16 nm) did not impact the ET efficiencies and neither did replacing the bicyclic diol site with a catechol derivative. Metadynamic analyses suggested that the conformations of the antennas are driven by intramolecular chromophoric stacking interactions. Upon forcing the α -helix to fold on itself, these interactions annul any effects deriving from the programming of the spatial arrangement of the receptor sides in the peptide backbone.

Provided that stable chromophores are used, these findings suggest that, to engineer efficient antennas following a template approach, one needs to select 1) templates featuring restrained conformational properties, 2) highly fluorescent chromophores, and 3) robust linkages that are chemically inert under the working conditions. It is with these guidelines that our activities will progress in the field, creeping ever closer to

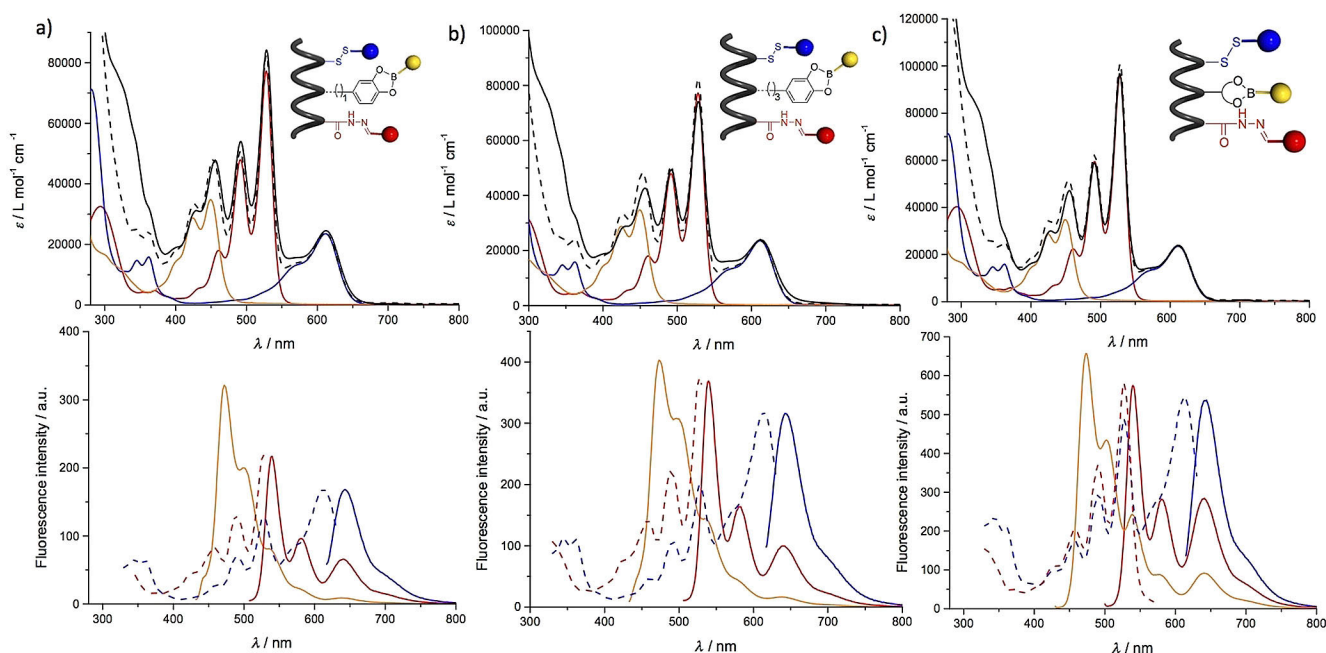


Figure 10. Top: Absorption spectra of antennas: a) RYB **30** (black solid line); b) RYB **31** (black solid line) normalized on B-NDI with arithmetic sum (dashed line) of absorption of dyes B-NDI (in blue), R-PDI (in red), Y-Per (in yellow) in DMF; c) RYB **23** (black solid line) normalized on B-NDI with arithmetic sum (dashed line) of absorption of dyes B-NDI (in blue), R-PDI (in red), Y-Per (in yellow) in DMA. Bottom: Emission (solid lines: $\lambda_{\text{exc}} = 423$ nm in yellow, $\lambda_{\text{exc}} = 495$ nm in red, $\lambda_{\text{exc}} = 609$ nm in blue), and corresponding normalized excitation spectra (dashed lines: $\lambda_{\text{emis}} = 540$ nm in red, $\lambda_{\text{emis}} = 640$ nm in blue) of antennas a) **30** and b) **31** in DMF, c) **23** in DMA.

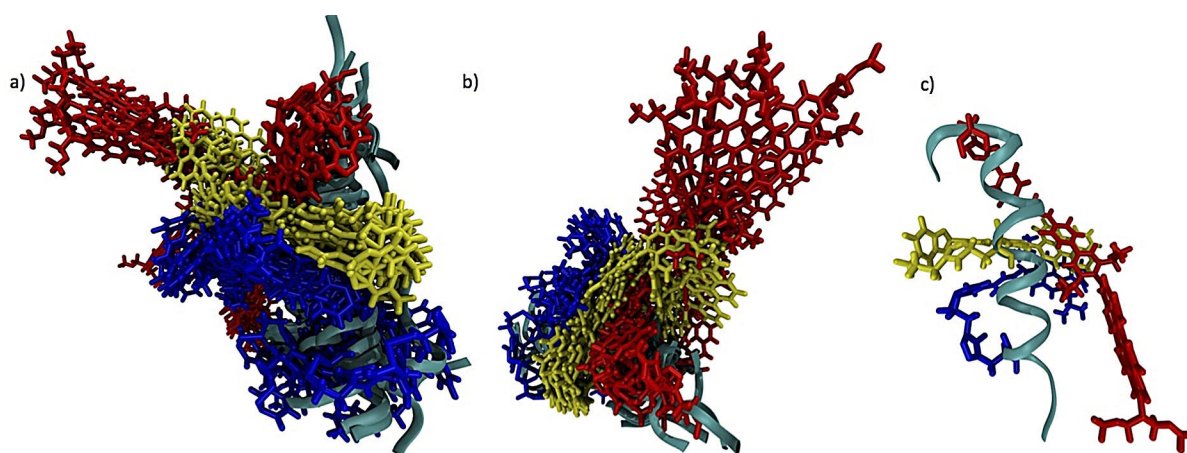


Figure 11. Metadynamics simulations of antenna **31** (100 ns); a) side and b) top view of overlaid frames; c) most stable conformation.

Table 2. Energy-transfer efficiencies within 23 in DMF and DMA.					
Entry	Peptide	Solvent	Methods	$\Phi_{\text{ET}}^{(\text{R-PDI} \rightarrow \text{B-NDI})}$ [%]	$\Phi_{\text{ET}}^{(\text{Y-Per} \rightarrow \text{B-NDI})}$ [%]
1	RYB 23	DMF	A: $\Phi_{\text{ET}} =$	21.9	7.7
			$QY_{\text{B-NDI}}^*/QY_{\text{B-NDI}}$	21.8	7.4
2	RYB 23	DMA	A	22	14
			B	22	15

the ultimate goal of developing artificial antennas with unitary light-harvesting efficiency.

Acknowledgements

D.B. and L.R. gratefully acknowledge the EU through the ERC Starting Grant "COLORLANDS" and ITN-ETN "PHOTOTRAIN" projects, as well as Cardiff University for the financial support.

The work has been performed using resources provided by the "Cambridge Service for Data Discovery" (CSD3, <http://csd3.cam.ac.uk>) system operated by the University of Cambridge Research Computing Service (<http://www.hpc.cam.ac.uk>) funded by EPSRC Tier-2 capital grant EP/P020259/1. We also thank A. De Leo for his contribution to the artwork.

Conflict of interest

The authors declare no conflict of interest.

Keywords: chromophores · energy transfer · metadynamics · peptide · self-assembly

- [1] a) N. Armaroli, V. Balzani, *Chem. Eur. J.* **2016**, *22*, 32–57; b) N. Armaroli, V. Balzani, *Energy Environ. Sci.* **2011**, *4*, 3193–3222.
- [2] a) R. E. Blankenship, *Molecular Mechanisms of Photosynthesis*, 2nd ed., Wiley-Blackwell, New York, **2014**; b) T. Mirkovic, E. E. Ostroumov, J. M. Anna, R. Van Grondelle, Govindjee, G. D. Scholes, *Chem. Rev.* **2017**, *117*, 249–293; c) P. D. Frischmann, K. Mahata, F. Würthner, *Chem. Soc. Rev.* **2013**, *42*, 1847–1870.
- [3] a) G. D. Scholes, G. R. Fleming, A. Olaya-Castro, R. Van Grondelle, *Nat. Chem.* **2011**, *3*, 763–774; b) R. Croce, H. Van Amerongen, *Nat. Chem. Biol.* **2014**, *10*, 492–501.
- [4] a) H. Q. Peng, L. Y. Niu, Y. Z. Chen, L. Z. Wu, C. H. Tung, Q. Z. Yang, *Chem. Rev.* **2015**, *115*, 7502–7542; b) S. Kundu, A. Patra, *Chem. Rev.* **2017**, *117*, 712–757; c) A. Harriman, *Chem. Commun.* **2015**, *51*, 11745–11756; d) L. Maggini, D. Bonifazi, *Chem. Soc. Rev.* **2012**, *41*, 211–241.
- [5] a) A. Kremer, E. Bietlot, A. Zanelli, J. M. Malicka, N. Armaroli, D. Bonifazi, *Chem. Eur. J.* **2015**, *21*, 1108–1117; b) K. Yoosaf, J. Iehl, I. Nierengarten, M. Hmadeh, A. M. Albrecht-Gary, J. F. Nierengarten, N. Armaroli, *Chem. Eur. J.* **2014**, *20*, 223–231; c) V. K. Praveen, C. Ranjith, E. Bandini, A. Ajayaghosh, N. Armaroli, *Chem. Soc. Rev.* **2014**, *43*, 4222–4242; d) N. Armaroli, G. Accorsi, J. N. Clifford, J. F. Eckert, J. F. Nierengarten, *Chem. Asian J.* **2006**, *1*, 564–574; e) D. Bonifazi, G. Accorsi, N. Armaroli, F. Song, A. Palkar, L. Echegoyen, M. Scholl, P. Seiler, B. Jaun, F. Diederich, *Helv. Chim. Acta* **2005**, *88*, 1839–1884; f) D. Bonifazi, M. Scholl, F. Song, L. Echegoyen, G. Accorsi, N. Armaroli, F. Diederich, *Angew. Chem. Int. Ed.* **2003**, *42*, 4966–4970; *Angew. Chem.* **2003**, *115*, 5116–5120; g) D. Bonifazi, F. Diederich, *Chem. Commun.* **2002**, 2178–2179.
- [6] S. S. Babu, D. Bonifazi, *ChemPlusChem* **2014**, *79*, 895–906.
- [7] a) A. Ajayaghosh, S. J. George, V. K. Praveen, *Angew. Chem. Int. Ed.* **2003**, *42*, 332–335; *Angew. Chem.* **2003**, *115*, 346–349; b) A. Ajayaghosh, V. K. Praveen, C. Vijayakumar, S. J. George, *Angew. Chem. Int. Ed.* **2007**, *46*, 6260–6265; *Angew. Chem.* **2007**, *119*, 6376–6381; c) A. Ajayaghosh, V. K. Praveen, C. Vijayakumar, *Chem. Soc. Rev.* **2008**, *37*, 109–122; d) C. Giansante, G. Raffy, C. Schafer, H. Rahma, M.-T. Kao, A. G. L. Olive, A. Del Guerso, *J. Am. Chem. Soc.* **2011**, *133*, 316–325; e) V. K. Praveen, C. Ranjith, N. Armaroli, *Angew. Chem. Int. Ed.* **2014**, *53*, 365–368; *Angew. Chem.* **2014**, *126*, 373–376.
- [8] a) R. Abbel, C. Grenier, M. J. Pouderoijen, J. W. Stouwdam, P. E. L. G. Leclere, R. P. Sijbesma, E. W. Meijer, A. P. H. J. Schenning, *J. Am. Chem. Soc.* **2009**, *131*, 833–843; b) H. Q. Peng, J. F. Xu, Y. Z. Chen, L. Z. Wu, C. H. Tung, Q. Z. Yang, *Chem. Commun.* **2014**, *50*, 1334–1337; c) A. Liang, S. Dong, X. Zhu, F. Huang, Y. Cao, *Polym. Chem.* **2015**, *6*, 6202–6207; d) C. B. Winiger, S. Li, G. R. Kumar, S. M. Langenegger, R. Haener, *Angew. Chem. Int. Ed.* **2014**, *53*, 13609–13613; *Angew. Chem.* **2014**, *126*, 13828–13832; e) Y. Kubo, R. Nishiyabu, *Polymer* **2017**, *128*, 257–275.
- [9] a) P.-Z. Chen, Y.-X. Weng, L.-Y. Niu, Y.-Z. Chen, L.-Z. Wu, C.-H. Tung, Q.-Z. Yang, *Angew. Chem. Int. Ed.* **2016**, *55*, 2759–2763; *Angew. Chem.* **2016**, *128*, 2809–2813; b) J. Sun, A. Klechikov, C. Moise, M. Prodana, M. Enacnescu, A. V. Talyzin, *Angew. Chem. Int. Ed.* **2017**, *56*, 10352–10356; *Angew. Chem.* **2017**, *129*, 10488–10492; c) V. Huber, S. Sengupta, F. Würthner, *Chem. Eur. J.* **2008**, *14*, 7791–7807; d) C. Röger, Y. Miloslavina, D. Brunner, A. R. Holzwarth, F. Würthner, *J. Am. Chem. Soc.* **2008**, *130*, 5929–5939.
- [10] a) C. Y. Lee, O. K. Farha, B. J. Hong, A. A. Sarjeant, S. B. T. Nguyen, J. T. Hupp, *J. Am. Chem. Soc.* **2011**, *133*, 15858–15861; b) H.-J. Son, S. Jin, S. Patwardhan, S. J. Wezenberg, N. C. Jeong, M. So, C. E. Wilmer, A. A. Sarjeant, G. C. Schatz, R. Q. Snurr, O. K. Farha, G. P. Wiederrecht, J. T. Hupp, *J. Am. Chem. Soc.* **2013**, *135*, 862–869.
- [11] a) R. S. K. Kishore, O. Kel, N. Banerji, D. Emery, G. Bollot, J. Mareda, A. Gomez-Casado, P. Jonkheijm, J. Huskens, P. Maroni, M. Borkovec, E. Vauthey, N. Sakai, S. Matile, *J. Am. Chem. Soc.* **2009**, *131*, 11106–11116; b) N. Sakai, M. Lista, O. Kel, S. I. Sakurai, D. Emery, J. Mareda, E. Vauthey, S. Matile, *J. Am. Chem. Soc.* **2011**, *133*, 15224–15227; c) G. Sforazzini, E. Orentas, A. Bolag, N. Sakai, S. Matile, *J. Am. Chem. Soc.* **2013**, *135*, 12082–12090; d) K.-D. Zhang, S. Matile, *Angew. Chem. Int. Ed.* **2015**, *54*, 8980–8983; *Angew. Chem.* **2015**, *127*, 9108–9111; e) K.-D. Zhang, N. Sakai, S. Matile, *Org. Biomol. Chem.* **2015**, *13*, 8687–8694.
- [12] a) M. S. Choi, T. Yamazaki, I. Yamazaki, T. Aida, *Angew. Chem. Int. Ed.* **2004**, *43*, 150–158; *Angew. Chem.* **2004**, *116*, 152–160; b) S. Hecht, J. M. J. Fréchet, *Angew. Chem. Int. Ed.* **2001**, *40*, 74–91; *Angew. Chem.* **2001**, *113*, 76–94; c) V. Balzani, G. Bergamini, P. Ceroni, E. Marchi, *New J. Chem.* **2011**, *35*, 1944–1954; d) X. Zhang, Y. Zeng, T. Yu, J. Chen, G. Yang, Y. Li, *J. Phys. Chem. Lett.* **2014**, *5*, 2340–2350; e) L. Flamigni, B. Ventura, C. C. You, C. Hippius, F. Würthner, *J. Phys. Chem. C* **2007**, *111*, 622–630.
- [13] a) R. Takahashi, Y. Kobuke, *J. Am. Chem. Soc.* **2003**, *125*, 2372–2373; b) P. Parkinson, C. E. I. Knappe, N. Kamonsutthipajit, K. Sirithip, J. D. Matichak, H. L. Anderson, L. M. Herz, *J. Am. Chem. Soc.* **2014**, *136*, 8217–8220; c) J. Creemers, R. Haver, M. Rickhaus, J. Q. Gong, L. Favereau, M. D. Peeks, T. D. W. Claridge, L. M. Herz, H. L. Anderson, *J. Am. Chem. Soc.* **2018**, *140*, 5352–5355; d) P. Parkinson, N. Kamonsutthipajit, H. L. Anderson, L. M. Herz, *ACS Nano* **2016**, *10*, 5933–5940; e) C. K. Yong, P. Parkinson, D. V. Kondratuk, W. H. Chen, A. Stannard, A. Summerfield, J. K. Sprafke, M. C. O'Sullivan, P. H. Beton, H. L. Anderson, L. M. Herz, *Chem. Sci.* **2015**, *6*, 181–189; f) P. Parkinson, D. V. Kondratuk, C. Menelaou, J. Q. Gong, H. L. Anderson, L. M. Herz, *J. Phys. Chem. Lett.* **2014**, *5*, 4356–4361; g) Y. Wu, R. M. Young, M. Frasconi, S. T. Schneebeli, P. Spenst, D. M. Gardner, K. E. Brown, F. Würthner, J. F. Stoddart, M. R. Wasielewski, *J. Am. Chem. Soc.* **2015**, *137*, 13236–13239.
- [14] a) A. Wilson, G. Gasparini, S. Matile, *Chem. Soc. Rev.* **2014**, *43*, 1948–1962; b) S. Lascano, K. D. Zhang, R. Wehlauch, K. Gademann, N. Sakai, S. Matile, *Chem. Sci.* **2016**, *7*, 4720–4724; c) H. M. Seifert, K. R. Trejo, E. V. Anslyn, *J. Am. Chem. Soc.* **2016**, *138*, 10916–10924; d) B. M. Matysiak, P. Nowak, I. Cvrtila, C. G. Pappas, B. Liu, D. Komáromy, S. Otto, *J. Am. Chem. Soc.* **2017**, *139*, 6744–6751; e) J. F. Reuther, J. L. Dees, I. V. Kolesnichenko, E. T. Hernandez, D. V. Ukraintsev, R. Guduru, M. Whiteley, E. V. Anslyn, *Nat. Chem.* **2018**, *10*, 45–50; f) Y. Jin, C. Yu, R. J. Denman, W. Zhang, *Chem. Soc. Rev.* **2013**, *42*, 6634–6654.
- [15] a) C. M. Spillmann, I. L. Medintz, *J. Photochem. Photobiol. C* **2015**, *23*, 1–24; b) Q. Zou, K. Liu, M. Abbas, X. Yan, *Adv. Mater.* **2016**, *28*, 1031–1043.
- [16] a) Y. N. Teo, E. T. Kool, *Chem. Rev.* **2012**, *112*, 4221–4245; b) P. Ensslen, H. A. Wagenknecht, *Acc. Chem. Res.* **2015**, *48*, 2724–2733.
- [17] a) H. Q. Peng, Y. Z. Chen, Y. Zhao, Q. Z. Yang, L. Z. Wu, C. H. Tung, L. P. Zhang, Q. X. Tong, *Angew. Chem. Int. Ed.* **2012**, *51*, 2088–2092; *Angew. Chem.* **2012**, *124*, 2130–2134; b) W. C. Geng, Y. C. Liu, Y. Y. Wang, Z. Xu, Z. Zheng, C. B. Yang, D. S. Guo, *Chem. Commun.* **2017**, *53*, 392–395.
- [18] a) K. V. Rao, A. Jain, S. J. George, *J. Mater. Chem. C* **2014**, *2*, 3055–3064; b) Z. M. Hudson, D. J. Lunn, M. A. Winnik, I. Manners, *Nat. Commun.* **2014**, *5*, 3372.
- [19] L. Rocard, A. Berezin, F. De Leo, D. Bonifazi, *Angew. Chem. Int. Ed.* **2015**, *54*, 15739–15743; *Angew. Chem.* **2015**, *127*, 15965–15969.
- [20] a) T. Förster, *Discuss. Faraday Soc.* **1959**, *27*, 7–17; b) P. Wu, L. Brand, *Anal. Biochem.* **1994**, *218*, 1–13.
- [21] P. G. Bolhuis, D. Chandler, C. Dellago, P. L. Geissler, *Annu. Rev. Phys. Chem.* **2002**, *53*, 291–318.
- [22] A. Laio, M. Parrinello, *Proc. Natl. Acad. Sci. USA* **2002**, *99*, 12562–12566.
- [23] a) Z. Sun, Q. Ye, C. Chi, J. Wu, *Chem. Soc. Rev.* **2012**, *41*, 7857–7889; b) J. T. Markiewicz, F. Wudl, *ACS Appl. Mater. Interfaces* **2015**, *7*, 28063–28085.
- [24] I. B. Berlman, *Handbook of fluorescence spectra of aromatic molecules*, Academic Press, New York, **1971**.
- [25] F. Würthner, *Chem. Commun.* **2004**, 1564–1579.
- [26] F. Würthner, C. Thalacker, S. Diele, C. Tschierske, *Chem. Eur. J.* **2001**, *7*, 2245–2253.

- [27] P. D. Frischmann, F. Würthner, *Org. Lett.* **2013**, *15*, 4674–4677.
- [28] É. Torres, M. N. Berberan-Santos, M. J. Brites, *Dyes Pigm.* **2015**, *112*, 298–304.
- [29] S. J. Coutts, J. Adams, D. Krolikowski, R. J. Snow, *Tetrahedron Lett.* **1994**, *35*, 5109–5112.
- [30] M. R. Hansen, T. Schnitzler, W. Pisula, R. Graf, K. Muellen, H. W. Spiess, *Angew. Chem. Int. Ed.* **2009**, *48*, 4621–4624; *Angew. Chem.* **2009**, *121*, 4691–4695.
- [31] R. Kota, R. Samudrala, D. L. Mattern, *J. Org. Chem.* **2012**, *77*, 9641–9651.
- [32] N. Sewald, H. D. Jakubke, *Peptides: Chemistry and Biology*, 2nd ed., Wiley-VCH, Weinheim, **2009**.
- [33] a) J. R. Lakowicz, *Principles of fluorescence spectroscopy*, 3rd ed., Springer, New York, **2006**; b) I. B. Berlman, *Energy Transfer Parameters of Aromatic Compounds*, Academic Press, New York, **1973**.

 Manuscript received: June 25, 2018

Accepted manuscript online: August 21, 2018

Version of record online: ■ ■ ■ ■. 0000

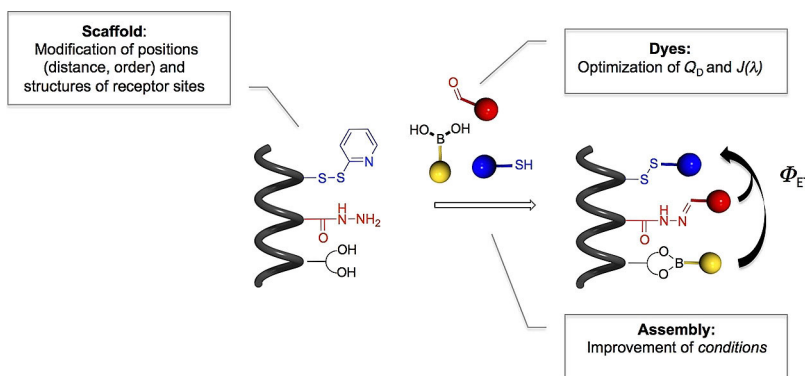
FULL PAPER

Self-Assembly

L. Rocard, D. Wragg, S. A. Jobbins,
L. Luciani, J. Wouters, S. Leoni,
D. Bonifazi*



 **Templated Chromophore Assembly on Peptide Scaffolds: A Structural Evolution**



Designing antennas: Investigation of α -helix peptides as templates for engineering light-harvesting antennas through a multichromophoric assembly approach is reported. The effect of vari-

ous structural parameters was studied and a significant improvement of the energy transfer across the chromophores was observed.